Petroleum 11 (2025) 638–652

Contents lists available at ScienceDirect

Petroleum

journal homepage: www.keaipublishing.com/en/journals/petlm

Full Length Article

Investigation of natural surfactant for oil recovery potential

Aibike Tukhfatova [a], Azza Hashim Abbas [b,*], Sonny Irawan [a], Peyman Pourafshary [a]

[a] Department of Petroleum Engineering, School of Mining and Geosciences, Nazarbayev University, Astana 010000, Kazakhstan
[b] Institue of Geoenergy Engineering, Heriot-Watt University, Edinburgh EH14 4AS, UK

ARTICLE INFO

Article history:
Received 11 September 2024
Received in revised form
27 February 2025
Accepted 2 September 2025

ABSTRACT

Advancing the use of natural surfactants in enhanced oil recovery is crucial for sustainable practices in the oil and gas industry. This research assesses the applicability of neem-derived natural surfactants in offshore fields, encompassing surfactant synthesis via saponification, characterization through FT-IR, SEM, and EDS, and measuring surface and interfacial tension across various conditions. Adsorption studies determined the surfactant's adsorption characteristics onto rock, and core flooding tests assessed its efficacy. Surface tension measurements in deionized water (DIW) and brine confirmed the surfactant's surface activity. As the concentration increased from 1 wt% to 6 wt%, the interfacial tension (IFT) significantly decreased from 22.5 mN/m to 7.9 mN/m, marking a 64.8% reduction. Additionally, surfactants formed micelles more efficiently in saline water, with the critical micelle concentration (CMC) dropping from 4.0 wt% in DIW to 0.9 wt%.Adsorption on limestone showed over 50% higher adsorption than sandstone, confirming stronger interactions and higher adsorption saturation. Core flooding experiments demonstrated the surfactant's effectiveness in oil and water-wet conditions. When injected into sandstone, the surfactant achieved a significant additional oil recovery of 24.6% in deionized water, compared to 10.2% in limestone. Conversely, in saline conditions, the surfactant's performance was better in limestone, achieving an additional recovery of 4.9%, whereas in sandstone, it was only 1.6%. This research offers a unique perspective on how natural surfactants perform across different rock types. The findings suggest that neem-derived surfactants hold significant promise for enhancing oil recovery in Kazakhstan's oil fields.

1. Introduction

Finding a chemical to reduce the footprint of synthetic chemicals is crucial in today's oil and gas industry. The mission involves “green synthesis” to enhance oil and gas recovery. This twofold approach requires cheap, environmentally friendly, and technically effective compounds [1,2]. Surfactants, polymers, or their combinations are key chemicals in all oil and gas practices. Their actions in the formation are usually described as chemical enhanced oil recovery (CEOR). Their dual action improves oil recovery by reducing mobility or increasing the capillary number [3,4].

Surfactants have been researched globally, with historical oil application discoveries dating back to the 1940s. Surfactant flooding, as a chemical oil recovery technique, injects surfactants into reservoirs to enhance microscopic sweep efficiency and increase oil recovery. It reduces interfacial tension (IFT) and modifies fluid/rock characteristics, improving oil mobilization and reducing residual oil saturation. One of the most common drawbacks of using surfactants is the potential creation of in-situ pressure, which is uncontrollable. Additionally, surfactants can form emulsions, leading to significant oil loss. However, the most significant drawback is their high cost, which limited their application in subsurface operations at the 50s and 60s [5,6]. During the 70s the stream was on coupling the surfactant performance to the polymer to improve the recovery which is beneficial [7–9]. In the 80s and 90s industry focused on using surfactants at very low concentrations [10].

Since the dawn of the new millennium, a new focus on biodegradable and cost-effective surfactants has led to the

---

* Corresponding author.
E-mail addresses: azzahashim2008@gmail.com, ahh4000@hw.ac.uk (A.H. Abbas).

Peer review under the responsibility of Southwest Petroleum University.

https://doi.org/10.1016/j.petlm.2025.09.001

exploration of natural surfactants. Natural surfactants, derived from renewable sources, offer a promising alternative to synthetic ones. They are environmentally friendly and biodegradable, reducing the environmental impact. Therefore, natural surfactants are increasingly favored for their green attributes. They are sourced from plants or animals and synthesized from raw materials, such as polyols and simple sugars [11–15]. Components extracted from plants containing saponins, such as leaves, roots, and bark, display natural surfactant properties [16–18]. They contribute to reducing the IFT, altering oil–rock surface contact angles, and influencing foaming and emulsification. These natural surfactants are derived without chemical reactions and can be directly applied after extraction without further processing. Previous studies have illuminated the different paths of natural surfactant application. A study conducted by Norouzpour et al. [13, 14] investigated a novel surfactant derived from quinoa for oil recovery. Their surfactant showed excellent thermal stability, higher emulsification ability, and reduced IFT, making it comparable with the commercial surfactants TR-880 and NX-610 [13]. Abbas et al. [19] examined the adsorption of three natural surfactants (saponins sourced from fenugreek, sugar beet leaves, and chickpeas) on rock surfaces. They found 192 g/kg adsorption at 5 wt% critical micelle concentration (CMC). The study focused on surface interaction, without phase analysis [19].

Oil recovery experiments have shown a 24.1% increase using natural surfactant flooding at 1500 ppm as tertiary recovery. Additionally, Nafisifar et al. [20] explored the synthesis of a novel anionic surfactant derived from linseeds, a natural base material. Applying the natural surfactant solution decreased the contact angle from 126° to 54.5°, transitioning the sandstone surface to a water-wet state and boosting oil recovery by 7.9% [20]. In their study, Zhao et al. [21] A study was conducted on a new eco-friendly surfactant extracted from green pea (Pisum sativum). The research revealed that optimal results were achieved when utilizing a solution containing 1500 ppm of the green surfactant and formation brine with 12,500 ppm salinity. Under these conditions, the contact angle and IFT reached their lowest values of 54.3° and 3.74 mN/m, respectively [21]. It is evident that the natural surfactant performance is influenced by different parameters such as oil type, salinity, temperature, source of the surfactant and reservoir rock interaction (Table 1). The research carried out to assess the efficiency of natural surfactants has been complex and has not provided conclusive answers to their limit.

Kazakhstan, with its significant large offshore oil fields, presents an underexplored opportunity for employing these eco-friendly and cost-effective methods. The authors' previous studies explored some aspects of readily available local natural materials or globally known sources [22–24]. This current study aims to explore the efficacy of natural surfactants in improving oil recovery in Kazakhstan's specific reservoir conditions. Given that chemicals should originate from readily available resources, the potential of neem as a surfactant is encouraging. Thus, the main objectives of the study are to synthesize a neem-based surfactant and evaluate its performance. The specific objectives include characterizing the developed natural surfactant and assessing the reduction in IFT under various salinities and temperatures. The research also highlights the expected surfactant losses caused by adsorption on reservoir rocks. The study provides insight into the natural surfactant performance in both water-wet and oil-wet cores utilizing seawater salinity. The research is a progression step in designing and optimizing surfactants by coupling chemical innovation with a high degree of physical understanding of complex reservoirs. This research confronts the mechanism and sensitivity challenges that have hampered novel natural surfactant progress in this field.

2. Methodology

The experiments focused on the use of a neem-derived surfactant for CEOR and included determining ST, IFT, characterization of active compounds, morphology, and elemental composition. Core flooding tests provided more details for the offshore application to examine the surfactant's displacement effectiveness under various conditions.

2.1. Materials

Neem powder is derived from the leaves of the Azadirachta indica tree, which is native to India and various regions across South Asia and Africa, and is used as an organic herbal remedy. It contains over 300 primary and secondary metabolites, including fats, carbohydrates, proteins, flavonoids, steroids, saponins, and alkaloids. This study utilized neem powder for its rich content of active elements, such as terpenoids and flavonoids, which enhance its surface-active properties, making it an effective surfactant enhancer. The neem powder used was sourced from “Africa Natural” and purchased online as a dried and ground product. Organic extra virgin olive oil, which was used in the study as a soaking medium, was obtained from local market in Astana, Kazakhstan.

The core samples of Indiana limestone and Berea sandstone from Texas, USA, dating to the Lower Cretaceous and Upper Devonian periods, respectively, were used to test the effectiveness of the surfactants developed in the study.

The synthetic oil known as decane, which had a purity level of 99% and a molecular weight of 142.28 g/mol, was used in the studies. The Sigma-Aldrich Company supplied this decane. Data from the Stabinger viscometer at temperatures ranging from 20 °C to 80 °C are shown in Table 2.

2.2. Synthesis of natural surfactant

To prepare the mixture, 50 ml of olive oil and 10 g of neem powder were combined in a container and allowed to soak for 18 h. This step ensured facilitating the diffusion of neem compounds by the olive oil.The diffusion occurs due to the oil solvent properties. After soaking, the mixture was sieved and heated to 50 °C-55 °C to initiate saponification by breaking down oil esters. During this phase, the mixture's color changed due to chemical reactions between neem compounds (such as terpenoids and flavonoids) and the olive oil. After heating, the precipitated neem powder was filtered out, and a 10 M sodium hydroxide solution was added. The solution was then stirred at 55 °C and 250 rpm until fully homogenized, ensuring a uniform mixture for successful saponification. The process is depicted in Fig. 1.

2.3. Preparation of surfactant solution

Six distinct solutions were prepared using surfactant powder and deionized water (DIW) to generate surfactant solutions with various concentrations. The concentrations ranged from 0.5 wt% to 6 wt% by weight. Each solution was positioned on a magnetic stirrer and stirred at a speed of 250 rpm until it achieved complete homogeneity. To investigate the salinity's influence, the surfactant was prepared in brine with NaCl at different concentrations within the 0.1–3.5 wt% range. Notably, the surfactant solutions exhibited stability throughout the experimentation period, with no indication of precipitation or degradation. The effect of temperature was addressed by varying the solution temperature from 35 °C to 55 °C.

Table 1
Recent research explores the utilization of natural surfactants in enhanced oil recovery.

Surfactant name	Rock type	Oil type	Temperature	Salinity	pH	Adsorption	Interfacial tension (IFT)	Key findings	Reference
Alfalfa plant	Dolomite & limestone	Kerosene & crude oil: 0.7998–0.8801 g/cm^3	N/A	Formation water	5.9	N/A	IFT reduction from 46.2 mN/m to 16.9 mN/m.	At the optimum concentration of 4 wt%, the surfactant in DW showed best results, with reductions of 63.4% in IFT and 49.9% in contact angle. Weaker impacts of sulfate & magnesuim ions compared with calcuim on IFT & contact angle reductions. Imbibition experiments indicated that 3Ca2 + SW + 4 wt% Alfalfa surfactant solution improved 62% of RF.	[25]
Vitagnus plant	Carbonate	API of the oil: 29^0	70 °C	N/A	4.69–5.95	N/A	IFT reduction from 29.5 mN/m to 5.28 mN/m.	5000 ppm of the plant extract based on deionized water (DIW) decreased IFT by 93.6% to 1.87 mN/m. Lowering the contact angle from 114° to 29° altered the surface of the carbonate from oil-wet to water-wet. Injecting 2 pore volume (PV) of the surfactant solution enhanced oil recovery from 44% to 56.8%.	[26]
Soapwort plant	Sandstone	API of the oil: 27.97^0	80 °C	FW, NaCl, $MgCl_2$: 5000–40,000 ppm	N/A	N/A	IFT reduction from 10.275 mN/m to 0.807 mN/m.	The introduction of the natural surfactant at different salinities reduced the contact angles by 35.12° (FW), 38.44° ($MgCl_2$), and 43.62° (NaCl).	[27]
Linseeds	Sandstone	Crude oil	130 °C	5000–160,000 ppm	7.9–8.2	8.21 mg/g	IFT reduction from 28.9 mN/m to 0.99 mN/m.	The contact angle decreased from 126° to 54.5°. Foam stability test indicated that at a 10 mL/s flow rate, the surfactant exhibits improved stability. At the CMC, flooding with surfactant at a concentration of 70,000 ppm NaCl yielded a 7.9% oil recovery.	[20]
Karanj oil	Sand pack	Crude oil: 6.22 mPa s at 50 °C/1.12 mg KOH/g	30^{0}C–70 °C	NaCl: 21 wt%, 23 wt%, 25 wt%	N/A	Effect of temperature: 30 °C: 3.68 mg/g 50 °C: 3.35 mg/g 70 °C: 2.97 mg/g Effect of polymer concentration: 500 ppm: 3.45 mg/g 1000 ppm: 3.21 mg/g 2000 ppm: 2.75 mg/g effect of salinity: 5000 ppm (0.5 wt%): 4.11 mg/g 10,000 ppm (1 wt%): 4.63 mg/g 20,000 ppm (2 wt%): 4.54 mg/g Effect of time: 1 day: 4.14 mg/g 2 days: 4.62 mg/g 3 days: 5.25 mg/g 4 days: Increase to 5.63 mg/g 5 days: peak adsorption observed at 5.63 mg/g	Critical micelle concentration (CMC) (8500 ppm) achieved the minimum IFT at 0.062 mN/m.	Achieved minimal IFT of 0.0081 mN/m at CMC (2 wt% salt). The surfactant solution in DIW decreased the contact angles from 127° to 79°-43° at 0.2 wt% & 0.85 wt%, respectively. Exhibited lower adsorption than conventional anionic surfactants. Extra oil recovery (24%–31%) was obtained with ASP slug applying the natural surfactant.	[28]

Myrtus communis plant	Carbonate	API of the oil: 31.14^0	75 °C	KCl, NaCl, $CaCl_2$, $MgCl_2$, Na_2SO_4, $MgSO_4$, K_2SO_4, KI: 5000–80,000 ppm	4.0–6.0	The minimum adsorption concentration was observed at 500 ppm, while the maximum rate occurred at 7000 ppm.	IFT decreased from 12.48 mN/m to 0.861 mN/m.	At CMC, the IFT drops significantly to 0.861 mN/m, and at optimum salinities and alkali concentrations, it reaches an impressively low value of 5.95×10^{-2}. Surfactant flooding enhanced oil recovery by 14.3%.	[29]
Albizia julibrissin plant	Carbonate	Kerosene 0.79 g/cm^3, crude oil 0.89 g/cm^3	N/A	N/A	7.06	N/A	IFT decreased from 34 mN/m to 10 mN/m.	The natural surfactant altered oil-wet carbonate rocks wettability from 165.02° to 86.59°, resulting in an 11.6% enhancement in tertiary oil recovery.	[30]
Vernonia amygdalina leaves	Sandstone	API of the oil: 37.7^0	N/A	NaCl: 0.9–3 wt%	N/A	N/A	IFT decreased from 18 mN/m to 0.97 mN/m.	The surfactant displayed a CMC at1 wt%, leading to a reduction in the IFT. The surfactant formed stable emulsions, lasting several hours. Changed the surface properties from being oil-wet to becoming water-wet. The contact angle was reduced from 118° to 45.7°.	[31]
Quinoa plant	Carbonate	API of the oil: 32.6^0	78 °C	N/A	6.29–6.50	N/A	IFT decreased from 33.2 mN/m to 8.7 mN/m.	Modified surface properties resulting in contact angles of 26.3° and 20° at 1500 and 5000 ppm. The alteration in surface properties shifted from oil-wet to water-wet. The surfactant showed the higher emulsification ability compared with commercial surfactants. Oil recovery experiments showed a 24.1% increase using natural surfactant flooding at 1500 ppm as tertiary recovery.	[13]
Tanacetum and tarragon plants	Carbonate	API of the oil: 29^0	70 °C	500–7000 ppm	N/A	N/A	5000 ppm of tarragon in DIW, the IFT dropped from 29.5 mN/m to 5.12 mN/m. In brine, the IFT decreased from 28 mN/m to 6.57 mN/m with 1000 ppm of tarragon.	DW based TAR-5000 & TAN-1000 demonstrated the better performance in decreasing of the contact agles of 30.8° & 33°. Tarragon and tanacetum surfactants enhanced oil recovery by 11.7% and 13.2% of OOIP post-waterflooding, respectively.	[32]
Fruit of sapindus mukorossi	Berea sandstone	API of the oil: 36.5^0	100 °C	1000–10,000 ppm	4.7 at 1 wt%, 4.42 at 6 wt%, 4.46 at 9 wt%	N/A	IFT decreased from 17.4 mN/m to 3.8 mN/m.	Raising salt concentration to 18,000 ppm stabilizes foam, and higher temperatures increase surfactant solubility, leading to increased foam height. Contact angle reduced from 52.1° to 22.03° at CMC. Reducing the salinity concentration led to a decrease in the contact angle from 35.40° to 24.30°.	[33]
Cashew nutshell liquid	Sandstone	API of the oil: 22.5^0	25^0C–80 °C	NaCl, ca, $MgCl_2$ TDS = 30,000 ppm; Ca and Mg concentrations 5000 mg/l (divalent ions)	5.2–6.4	N/A	IFT decreased from 10.46 mN/m to 1.66 mN/m.	At laboratory temperature, recovery is 12 % OOIP and a displacement efficiency is 32.5%. At 80 °C, the recovery is 9% OOIP and a displacement efficiency is 25%.	[34]

Table 2
Measured synthetic oil characteristics at various temperatures.

Cell Temperature/°C	Kinamatic viscosity/cP	Density/g·cm^{-3}
20	0.91	0.733
30	0.78	0.725
40	0.65	0.718
50	0.59	0.710
60	0.53	0.702
70	0.47	0.602
80	0.40	0.547

2.4. Material characterization

The prepared surfactant was analyzed for its functional groups and structural confirmation using Fourier-transform infrared (FTIR) spectroscopy, a scanning electron microscope (SEM), and energy dispersive spectrum (EDS) analysis. Using a Nicolet iS10 FTIR spectrometer (Massachusetts, US) equipped with a ZnSe flat crystal, the analysis commenced by collecting and comparing background spectra against reference backgrounds for each sample. Following this, 20 mg of crushed and powdered samples were applied to the crystal, and spectra were obtained through 32 transmission scans spanning the spectral range of 4000–400 cm^{-1}, with a resolution of 4 cm^{-1}. An SEM is a high-resolution microscope used to generate detailed pictures of the sample structure. A detailed image of the sample was taken by adjusting the resolution and position as necessary. The SEM used in this study was the Zeiss Crossbeam 540 by Zeiss Group from Jena, Germany.

The sandstone and limestone employed in this study were crushed into a powder state through a two-stage process. Initially, the samples were broken into fragments <20 mm using a Jaw Crusher machine by RETSCH (Germany). These fragments were then ground into micrometric particles using a RETSCH Disc Mill device. The cores were ultimately transformed into powders, serving as the material for the characterization. Brunauer–Emmett–Teller (BET) surface area analysis is a multi-point technique used to determine a material's specific surface area (m^2/g) through gas adsorption analysis. The BET tests were conducted using an Autosorb iQ Station 1 device. The researchers also used powder X-ray diffraction (XRD) equipment (Rigaku, Japan) to confirm the mineral composition. CuKα radiation was used for XRD analysis on the SmartLab (Rigaku) X-ray diffraction system. For the XRD analysis, the limestone and sandstone were ground further in an agate mortar and analyzed in the range of 2 Theta (10°–90°) The SEM was used in the same way as for the surfactants mentioned earlier.

2.5. Surface tension and interfacial tension measurement

Two devices were used to measure the ST and IFT of surfactant solutions: the K6 force tensiometer and the IFT 700-HPHT interfacial tension meter, respectively, as seen in Fig. 2. The K6, developed by KRÜSS in Hamburg, Germany, uses the ring detachment method to assess the ST at various concentrations and temperatures (45 °C, 55 °C, and 65 °C). It was also applied to seawater samples with 3.5 wt% NaCl. The IFT device, from Vinci Technologies in Nanterre, France, employs the pendant drop method based on the Laplace equation to determine the IFT across surfactant concentrations. The impact of salinity and temperature was determined to understand the parameters' effect on the surfactant/oil interface, from 1 to 6 wt% and seawater salinities of 0.1–3.5 wt%. Equipped with manual pumps, temperature sensors, and a control panel, it accurately adjusts conditions to study the temperature impact on IFT, which is essential for optimizing oil recovery processes.

2.6. Static adsorption quantification

Four grams of the crushed rock samples were mixed with 40 mL of surfactant solutions prepared in seawater salinity ranging

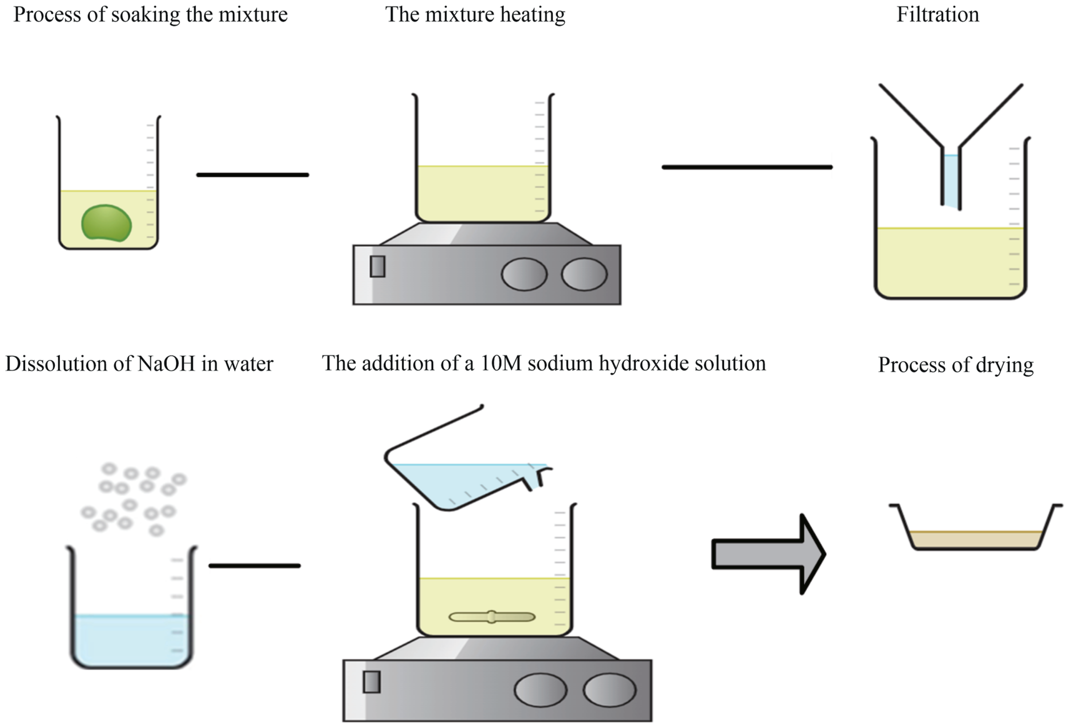

Fig. 1. Step-by-step process of combining neem compounds with olive oil to produce an esterified neem surfactant.

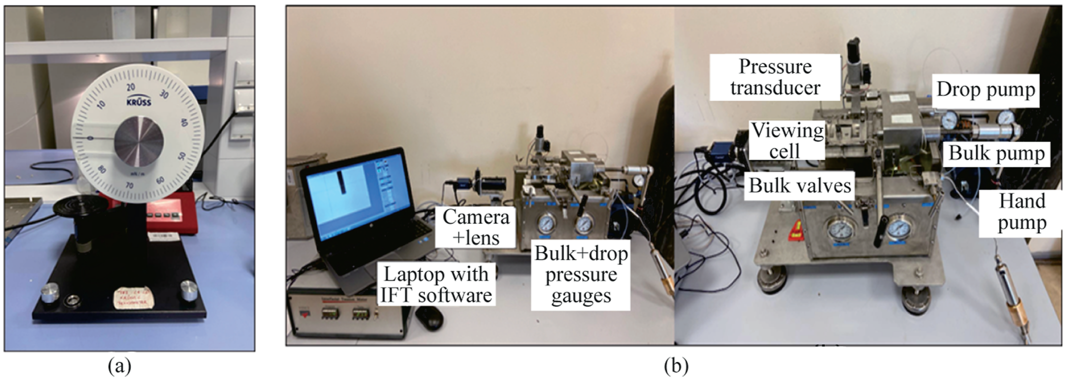

Fig. 2. Measuring devices: (a) surface tension tensiometer K6, (b) IFT 700-HPHT interfacial tension meter.

in concentration from 0.005 wt% to 6 wt%. The adsorption study focused on offshore salinity due to the diminishing expectancy of surfactants, as reported by several authors.

The mixtures were stirred at 100 rpm for 10 h using an IKA RH digital S000 magnetic stirrer. After stirring, the samples were separated using an Eppendorf 5702 centrifuge, operating at 4000 rpm for 5 min. The liquid collected from the upper portion after centrifugation was subjected to analysis using an ultraviolet–visible spectrophotometer (Evolution 300 by Thermo Scientific). Ultraviolet–visible spectrophotometry is a method for analyzing samples by measuring how they absorb or transmit ultraviolet and visible light, allowing for the determination of the concentration of elements or compounds present. The surfactant solution's highest peak was at 244 nm.The variation of concentrations used to develop surfactant solution calibration curve is presented in the supplementary file. The concentration levels post-adsorption were accurately deduced by employing calibration curves, providing insights into the adsorption dynamics at play. The adsorption amount was calculated using Eq.(1)

$$q = \frac{C_i - C_{ef}}{W} \times 1000 \tag{1}$$

q :adsorption amount (g/kg);
C_i: initial concentration (g/L);
C_{ef}: effluent concentration (g/L);
$V_{surfactant}$: volume of surfactant (mL);
$W_{adsorbent}$: weight of adsorbent (g).

2.7. Core flooding

Two cores were used for the core flooding tests. The injection of surfactant into both sandstone and limestone cores was chosen to assess its effectiveness under two known wettability conditions as previously stated [23]. Sandstone formations are typically water-wet, where water naturally adheres to the rock surface, whereas limestone formations are primarily oil-wet, with oil exhibiting a stronger affinity for the rock surface.

The dry weights and dimensions of the cores were recorded. In subsequent stages, the core samples were saturated with both brine and DIW-depend on the study condition-, depending on the type of salinity test. The core flooding test was conducted under these two conditions. The saturation procedure persisted for a day under a pressure of 1000 psi. After removing the cores from the apparatus, their wet weights were assessed to determine porosity. The manual saturationator from Vinci company, as illustrated in Fig. 3(a), was utilized for the saturation process. Both the sandstone and limestone remained merged to establish their wetting system.

The ACA-700 Aging Cell apparatus, supplied by Vinci Technologies in France, was employed in the subsequent trial. The process

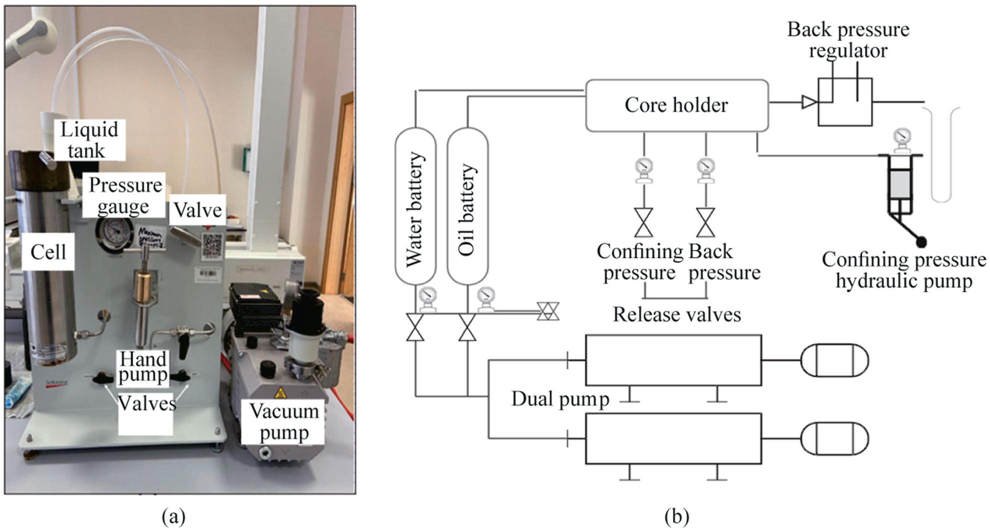

Fig. 3. (a) manual saturator; (b) ACA-700 aging cell equipment schematic.

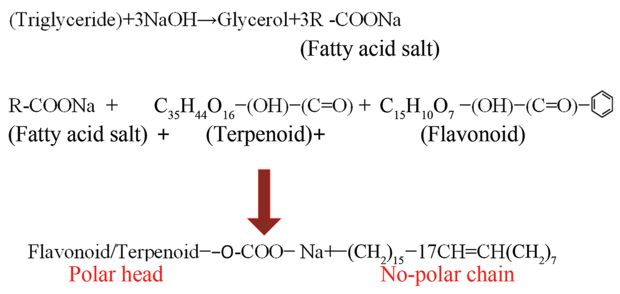

Fig. 4. Schematic of the generation of the natural surfactant.

followed what have been conducted earlier in our labs [23]. The components of the device are depicted in Fig. 3(b). Initially, DIW, brine, and decane were injected into the core at five varying flow rates: 0.5, 0.75, 1, 2, 3, 4, and 5 mL/min. This procedure was conducted to assess both the porosity and the absolute and effective permeability values utilizing Darcy's equation. The flooding process was initiated by injecting 1 pore volume (PV) of decane, which was succeeded by 5 PVs of DIW and brine to displace the oil. This aimed to calculate the initial oil recovery factor through water flooding. Following this, a surfactant solution at the CMC was introduced at a rate of 1 PV, which was succeeded by injecting 5 PVs of DIW and brine. Using these procedures, the total oil recovery factor was assessed. Throughout these stages, a consistent flow rate of 1 mL/min was maintained.

3. Results and discussion

3.1. Saponification and characterization of natural surfactant

Neem leaves contain a wide range of chemical compounds, both non-polar and polar. Firstly, they consist of alkanes and alkenes, which are non-polar. This compound can interact with long hydrocarbon chains in olive oil through van der Waals forces. Secondly, since neem is rich in hydroxyl groups (-OH) from phenols, flavonoids, and alcohols, and carbonyl groups (C=O) from ketones or aldehydes [35], the most significant interaction occurs between the hydroxyl groups of neem and the carboxyl groups of olive oil. The previous interactions happens during the soaking and heating period. The long carbon chains present in olive oil contribute to the hydrophobic tail of the surfactant, which is essential for surface activity. On the other hand, the bioactive compounds in neem, particularly the hydroxyl and carbonyl groups, are incorporated into the surfactant head. However, the typical saponification reaction means that the oil mixture underwent a chemical transformation to produce ester salts. This interaction between fatty acids in neem-infused olive oil and sodium hydroxide produces sodium (Na) salts of fatty acids. This reaction can be expressed as depicted in Fig. 4.

Yet, at this step, gaining insights and confirming the differences in the chemical attributes is vital. Thus, Fourier-transform infrared spectroscopy was utilized to identify the functional groups in olive oil and the newly developed neem natural surfactant. The FTIR results are presented in Fig. 5. The infrared absorption spectrum of olive oil displays peaks at 2921 cm^{-1} and 2852 cm^{-1}, indicative of C–H stretching vibrations common in the hydrocarbon chains of triglycerides. Another significant peak at 1743 cm^{-1} corresponds to C=O stretching, typical of carbonyl groups in fatty acids or esters. Peaks at 1117 cm^{-1} and 1159 cm^{-1} suggest C–O stretching, associated with ether or alcohol groups. These findings are consistent with the composition of olive oil, primarily made up of triglycerides, which are glycerol esterified with three fatty acids, aligning with prior FTIR studies on various oils [36,37].

The infrared spectrum of neem surfactant exhibits peaks at 3025.1 cm^{-1}, 2921.57 cm^{-1}, and 2849.19 cm^{-1}, indicating C–H stretching in alkene and alkane groups. Peaks at 1600 cm^{-1} and 905.9 cm^{-1} suggest C=C stretching, typical of alkene groups found in neem's limonoids and flavonoids. Additional peaks at 1492.25 cm^{-1} and 1451.53 cm^{-1}, and 1068.49 cm^{-1} and 1027.57 cm^{-1} point to alkane and ether or alcohol functional groups, respectively. Monosubstituted benzene and halo compounds are noted at 748.89 cm^{-1} and 538.01 cm^{-1}, corroborating findings in Hawsah et al.

The presence of alcohol groups in the surfactant indicates potential hydrophilicity, while alkane and alkene groups suggest hydrophobic properties. From previous findings by Nwanekezie et al. [35] and current study, neem and neem surfactant possess functional groups (O–H, C–H, C=O). This suggests successful integration of the functiona group into the produced surfactant. Furthermore, the absence of C=O- which is a component of neem bioactive compounds[38,39] and olive oil[40], implies chemical interaction of esters during saponification. Table 3 presents a comparison of the chemical compositions of olive oil and neem natural surfactants. This combination of hydrophilic alcohols and polar compounds with the hydrophobic alkane chains from olive oil demonstrates the successful formation of a balanced surfactant.

The FTIR results corroborate the saponification method described by Ogunkunle et al. [41], emphasising the suitability of

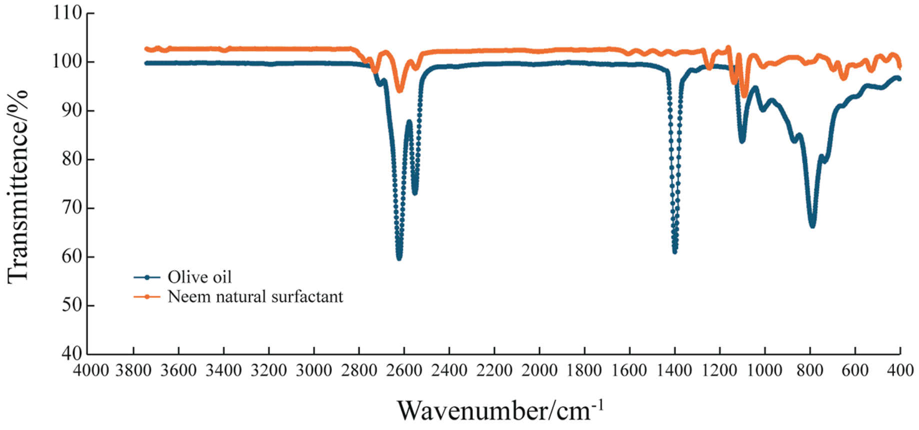

Fig. 5. Fourier-transform infrared spectroscopy results for the olive oil and natural surfactant derived from neem.

Table 3
Comparison of Fourier-transform infrared spectroscopy results.

Peak No.	Functional group	Compounds	Olive Oil	Neem-natural surfactant
Peak 1	O–H stretching	Alcohol	–	3025.1
Peak 2	C–H stretching	Alkane	2921.97	2921.57
Peak 3	C–H stretching	Alkane	2852.78	2849.19
Peak 4	C=O stretching	Esters	1743.46	Weak (1700–1750)
Peak 5	C=C			1600.77 (C=C stretching, conjugated alkene)
Peak 6	C–H Bending	Alkane	–	1492.25
Peak 7	C–H Bending	Alkane	–	1451.53
Peak 8	C–O stretching	Tertiary alcohol, vinyl ether	1159.65	1068.49
Peak 9	C–O stretching	Aliphatic ether, vinyl ether	1117.9	1027.57
Peak 10	C=C Bending	Alkene	–	905.9
Peak 11	C–H Bending	Monosubstituted benzene derivative	–	748.89
Peak 12	C–I stretching	Halo compound	–	538.01

neem oil for surfactant synthesis due to its fatty acid content [41]. De Azevedo Sá et al. [42] further demonstrate the efficacy of saponified neem oil as a natural hospital detergent. Despite methodological variations, these studies collectively underscore the potential of neem-based surfactants, highlighting the necessity for additional research to validate their applications [42].

As seen in Fig. 6(a), the natural surfactant was examined using the SEM at 100 × magnification, revealing a distinctive irregular flake-like morphology with sizes ranging from 30 μm to 500 μm. These variations from dense to crumbly textures suggest a complex compound composition. The surfactant's high surface area, indicated by its rough texture, enhances functionality by improving interactions with liquids, potentially boosting its ability to reduce ST and form micelles. The SEM images of the natural surfactant derived from neem displayed similarities to those documented in previous studies. In their research, Das et al. analyzed SEM micrographs of neem leaf powder. The images revealed that the powder comprised fine particles lacking a regular, uniform shape and size. These particles exhibited broken edges with steps and kinks, contributing to an uneven topography. The surface displayed a fibrous appearance with irregular macro-pores and some expanded cavities. During the EDS analysis of the natural surfactant, three elements were detected, namely carbon (C), oxygen (O), and Na, as illustrated in Fig. 6(b). In the EDS analysis of a natural surfactant derived from neem, the prevalence of C and O elements can be explained by the composition of the surfactant. The natural surfactant has organic properties, contributing to the sample's high C and O content. This observation aligns with the organic nature of the neem derived surfactant. The presence of Na is consistent with a Na salt of the fatty acid ester. The presence of Na suggests that the surfactant molecules have been saponified and the fatty acid esters have been converted to their Na salts, giving them anionic properties in aqueous solutions.

3.2. Characterization of reservoir cores

Fig. 7 shows X-ray diffraction patterns of limestone and sandstone. The X-ray diffraction pattern of limestone shows a calcite diffraction peak at 29° of high intensity, and the stone has a crystalline structure. For the sandstone, the peak at 26° is attributed to quartz. The pattern intensity of sandstone has a peak higher than that of limestone, indicating its higher crystallinity. Fig. 8 demonstrates the SEM images of the limestone and sandstone rock samples. As seen in Fig. 8, both samples reveal surfaces with a granular texture. In Fig. 8(a), the limestone shows predominantly angular grains and homogeneous sizes and shapes. The sandstone features grains that are less homogeneous, with angular edges. The angularity and rough surface texture suggest a higher mechanical strength and less chemical alteration. The BET analysis reveals that the specific surface area of limestone is 1.423 m^2/g, while that of sandstone is 1.506 m^2/g. This indicates that limestone has a smaller specific surface area compared with sandstone. The results confirm what was previously reported in the literature [43].

3.3. Surface tension and interfacial tension measurement

In oil and gas, a key characteristic of surfactants is their capacity to lower the IFT between the two existing phases. Before core flooding experiments, verifying surfactant effectiveness via ST measurements is vital. Successful reduction below water's typical

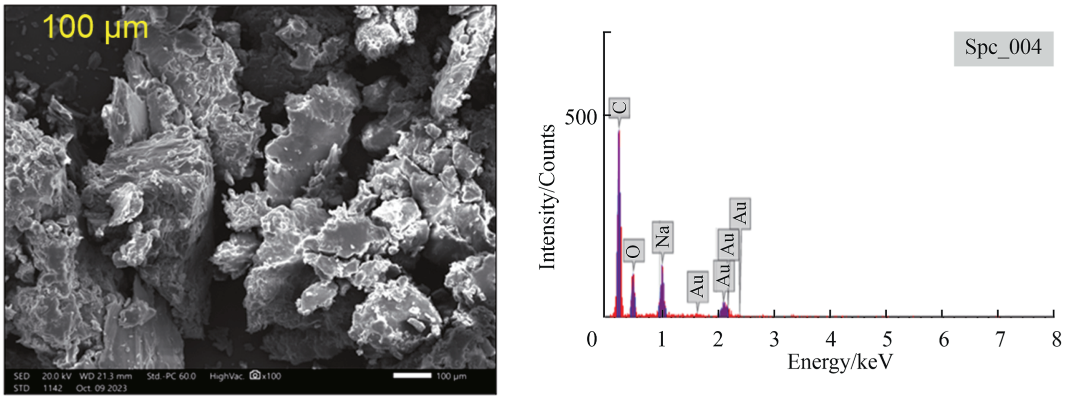

(a) (b)

Fig. 6. (a) natural surfactant scanning electron microscope image, (b) natural surfactant energy dispersive spectrum.

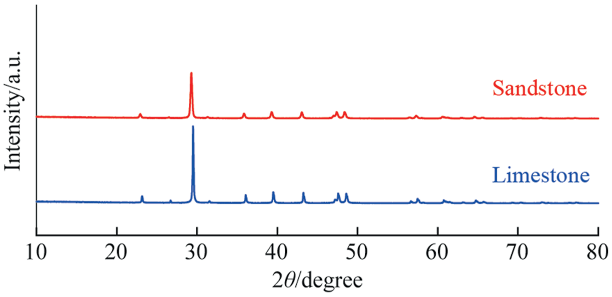

Fig. 7. X-ray diffraction results of sandstone and limestone.

tension of 72 mN/m—ideally <40 mN/m—indicates potential for EOR. This observation is associated with potential surfactant studies during the surface tension measurements [44–46]. In Fig. 9, the results show how the surfactant concentration and temperature influence ST in DIW and brine. The data show three distinguishable trends. In DIW, surfactants reduce ST with increasing concentration until reaching a plateau. With rising temperatures, the ST decreases for all concentrations. Conversely, in high salinity—crucial for offshore oil and gas operations—a different pattern emerges. Surface tension is generally lower than in DIW, but more dispersed at high surfactant concentrations, reflecting thermodynamic interactions in saline conditions. At high temperatures (55 °C and 65 °C), the ST difference between surfactant samples in DIW and saline is minimal, indicating effectiveness in reducing ST in both environments. This supports the narrative of natural surfactant stability. Statistically, at 25 °C, surfactants show a substantial reduction in ST of 7.57 mN/m, suggesting a significant impact of salinity. At 45 °C, the reduction is moderate, averaging 3.11 mN/m. At higher temperatures (55 °C and 65 °C), the reduction becomes smaller, averaging 2.72 mN/m and 2.28 mN/m, respectively. This trend was observed earlier in many types of surfactants [18,47–49]. In previous studies, the natural olive oil surfactant classified as non ionic surfactant offers only ST of 27 mN/m [50]. However, the current study improved the activity by utilizing the neem active compounds. The difference is attributed to the balanced hydrophilic-lipophilic structure in the non ionic surfactant, which is not the case when the additional hydrophilic groups such as hydroxyls from flavonoids is in neem anionic surfactant.

Increasing surfactant concentrations influences the IFT between oil and water. Although reducing IFT is crucial in EOR methods, because it facilitates the release and mobilization of trapped oil, it still relies on the concentration of surfactant available in the interface. Fig. 10 illustrates the IFT results obtained from the neem-derived surfactant solutions. Similarly, increasing the concentration of the natural surfactant from 1% to 6% resulted in IFT reduction. The decrease is from 22.5 mN/m to 7.9 mN/m, representing a remarkable 64.8% reduction. In seawater salinity, the reductions goes from 12 mN/m to 1.9 mN/m, representing 84.2%. Previous study by Saw et al., [50], upon introduction of the nonionic surfactant of olive oil, the olive oil-nonionic surfactant mixture exhibited elevated IFT values (19–20 mN/m) at a low concentration of 0.004 wt%. However, the efficacy of the surfactant is constrained by the complexity of the crude oil. In this study, the

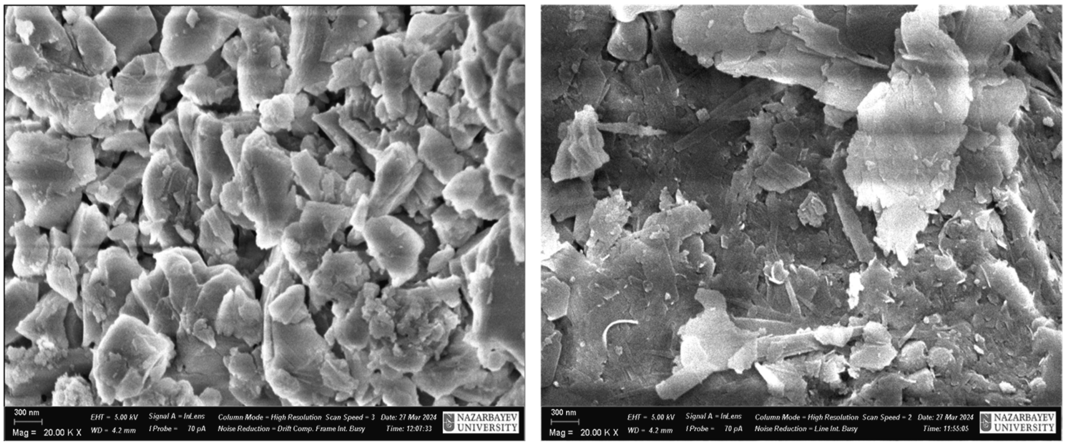

(a) (b)

Fig. 8. Scanning electron microscope images under 20 K magnification: (a) limestone, (b) sandstone.

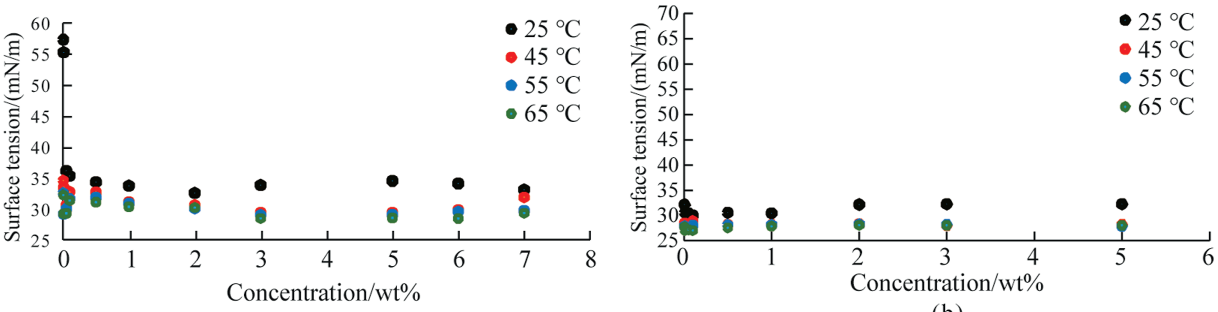

(a) (b)

Fig. 9. Natural surfactant surface tension measurement under reservoir temperature: (a) deionized water (no salinity) and (b) seawater salinity (3.5 wt% NaCl).

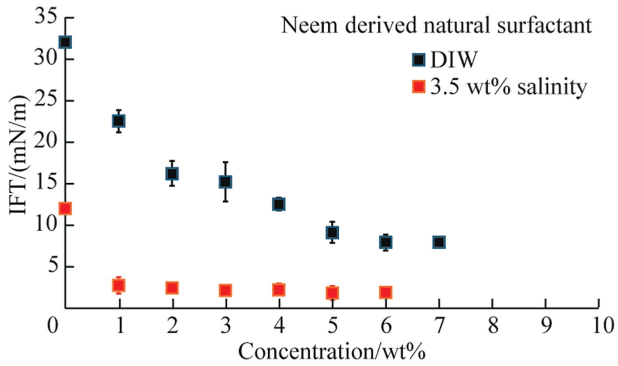

Fig. 10. The interfacial tension (IFT) values for the natural surfactant change with varying concentrations.

bioactive compounds in the neem surfactant may potentially further reduce IFT by providing additional surface-active effects, considering the oil utilized is not complex. Generally, anionic surfactants exhibit stronger electrostatic repulsion between surfactant molecules, leading to improved packing at the interface and consequently reducing IFT. Moreover, according to earlier studies, saponins extracted from quinoa resulted in a substantial 73.8% change in the IFT [13]. Furthermore, the surfactant obtained from linseeds decreased the IFT from 28.9 mN/m to 0.99 mN/m, indicating a decrease of 96% [20]. In the study by Khayati et al. [51], pure saponin's surfactant significantly reduced the IFT between kerosene and water from 30.4 mN/m to 9.9 mN/m. This study aligns with these findings, showing a similarly high IFT alteration yet not to the level of ultra low IFT. Referring back to the literature, the importance of reducing IFT is linked to increased oil recovery through various mechanisms, including capillary trapping depreciation, wettability alteration, and improvement in microscopic and macroscopic oil displacement within the reservoir. In calculations, the parameters affecting the capillary number remain the same except for the IFT. The rise in the capillary number due to the decrease in IFT from 22.5 mN/m to 7.9 mN/m is 1.235×10^{-6}, indicating a percentage increase of approximately 183%. This substantial increase proves the impact of the IFT reduction.

The CMC for surfactants varies between DIW and high salinity conditions. In DIW, the CMC is 4.0 wt%, indicating the threshold for micelle formation. In seawater salinity (3.5 wt%), the CMC drops to 0.9 wt%, showing a lower CMC due to the salinity's effect. The significant reduction in CMC suggests enhanced micelle formation efficiency, making surfactants more effective at lower concentrations compared with DIW. This indicates that surfactants require lower concentrations to achieve optimal performance in saline environments, which is crucial for offshore EOR applications. The mechanism under high concentrations of NaCl results in a more pronounced reduction in the IFT value. This is attributed to NaCl's impact on the electrical double layer at the interface, which screens charged groups on surfactant molecules. Consequently, repulsive forces diminish, promoting surfactant adsorption at the boundary and decreasing IFT.

3.4. Effect of salinity on oil/natural surfactant interfacial tension

As surfactants need to be compatible and tolerant of formation water, it is imperative to explore the impact of salt concentration on natural surfactants. The addition of salt can either be positive or negative on the IFT depending on surfactant concentration. As observed in Fig. 11, the relationship between surfactant concentration and varying salinity affecting the IFT is demonstrated. Increasing salinity reduces IFT in comparison to non-saline conditions. The interplay between ionic strength and surfactant concentration is evident. For instance, at low ionic strength less than 1.5 wt% NaCl, IFT decreases in all cases. However, when ionic strength exceeds surfactant concentration at the oil-water interface, the repulsion forces and IFT increase. For offshore applications, particular attention is given to the 3.5 wt% salinity. At higher surfactant concentrations such as 5 wt%, the IFT increases again at higher salinity of 3.5 wt% NaCl. This phenomenon can be attributed to the salting-out effect, wherein excessive salt concentration causes surfactant molecules to aggregate. The distribution of surfactant molecules across the oil and aqueous phases is salinity-dependent; at low salinity levels, predominant dissolution in the aqueous phase occurs, whereas high salinity promotes an affinity towards the oil phase [51]. Optimum salinity is achieved when surfactants are equitably solvated within both phases, facilitating the minimum achievable IFT [52].

In terms of the mechanism, increasing the concentration of NaCl demonstrates a more pronounced reduction in the IFT value. This increased impact is because the natural surfactantis inclined to be anionic. This signifies a similar role to the anionic surfactant/salinity/IFT condition. It is believed that the addition of NaCl influences the electrical double layer at the interface, screening charged groups on surfactant molecules. This diminishes repulsive

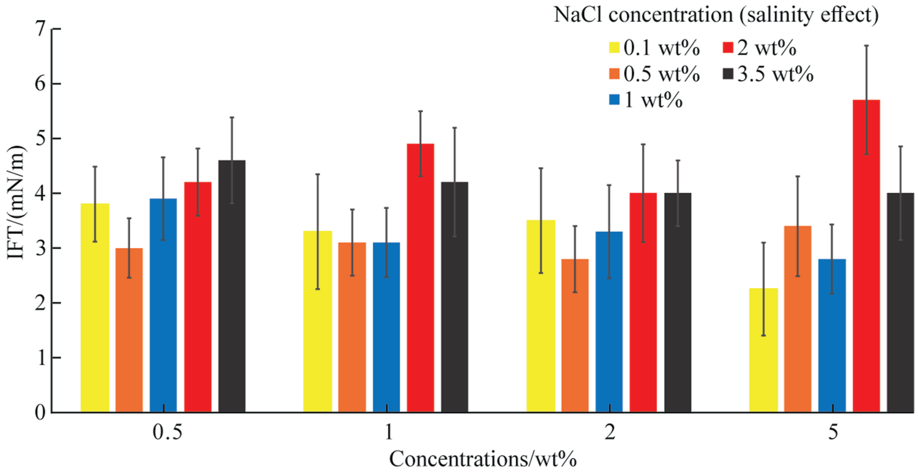

Fig. 11. Effect of salinity concentration on natural surfactant at different concentrations.

forces, facilitating surfactant adsorption at the interface and decreasing IFT.

3.5. Effect of temperature on oil/natural surfactant interfacial tension

A high temperature is helpful if the target is to solubilize oil by thermal methods; however, it is a significant disadvantage when it comes to chemical flooding. It is well established in the literature that chemicals break down under high temperatures. In the case of surfactants, dual roles have been reported. Some surfactants, such as anionic surfactants, lose their functionality under high temperatures, and accordingly, they cannot reduce the IFT to the desired limit. Other classes of surfactants can tolerate the temperature, but the required concentration increases to reach the targeted IFT. Moreover, all classes of surfactants adsorb less on rock surfaces. Thus, studying the impact of temperature can provide insights into the surfactants' thermodynamic stability.

The study involved measurements at various temperature levels representing temperature in Kazakhstan offshore. Fig. 12 shows that IFT initially decreases sharply as surfactant concentration rises to 1 wt%. This demonstrates effective IFT reduction at low surfactant levels.As the concentration increases, IFT values are steady. This indicates that there is a minimal change with increasing concentration. The slight variations in IFT at different temperatures suggest that temperature has little effect on the surfactant's ability to reduce IFT within the tested range. The overall trend indicates that the surfactant maintains its effectiveness across the temperature spectrum examined. However, by observing the high concentrations, it is more likely that increasing the temperature reduces the IFT.

Higher temperatures improve the natural surfactants' capacity to lower IFT, and this enhancement is due to the elevated temperatures facilitating superior surfactant adsorption at the oil–water interface, resulting in decreased IFT. As the temperature increases, the IFT between solutions containing anionic surfactants and crude oil decreases. Elevated temperatures boost the effectiveness of surfactant molecules at the interface. Increased mobility of these molecules elevates the overall entropy of the surface, leading to a decrease in its free energy, resulting in a lower IFT value.

3.6. Neem-derived surfactant adsorption under seawater salinity

One significant challenge in surfactant applications for EOR is surfactant adsorption on rock surfaces. Although adsorption can sometimes alter rock wettability beneficially, it often reduces the available surfactant for reducing the IFT. The problem is complex because in water-wet systems, the wettability alteration is not the crucial mechanism. In the current assessment, the adsorption on reservoirs dominated by sandstone (quartz) and limestone (calcite) was investigated. Moreover, given the use of seawater in EOR, it is essential to quantify surfactant loss under this condition. Ultraviolet spectrometer studies and static adsorption calculations reveal that low surfactant concentrations did not result in only significant adsorption but fully diminished the natural surfactant, as seen in Fig. 13. However, adsorption saturation reached higher concentrations, particularly on limestone, which showed over 50 % higher adsorption than sandstone. This is attributed to be highly hydrophobic characteristics, which further promotes the interaction. Furthermore, the natural surfactant may be more anionic, making it adsorb on limestone in a higher capacity than sandstone. The contribution of ionic strength can be added to the explanation of the well-known mechanism of electrostatic interaction. For instance, the water often has an ionic strength of 0.001–0.1 mol/L, whereas the current study has a high ionic strength of 0.599 mol/L.

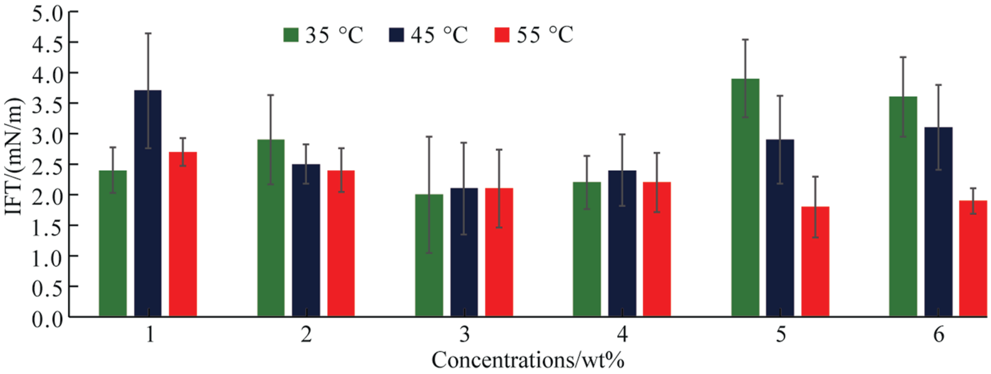

Fig. 12. Effect of temperature on natural surfactants at different concentrations.

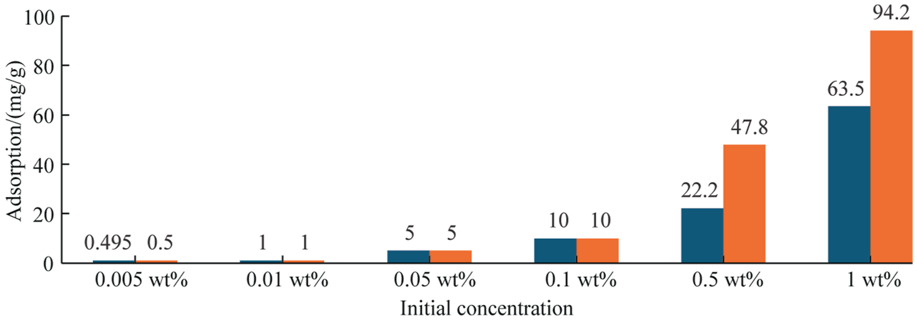

Fig. 13. Impact of surfactant adsorption on sandstone and limestone samples.

Therefore, high ionic strength reduces the electrostatic repulsion and promotes anionic surfactant adsorption on negatively charged quartz. Conversely, an increased salinity enhances electrostatic attraction with anionic surfactants for positively charged calcite, increasing the adsorption [53,54].

3.7. Application of neem-derived surfactant in oil recovery

The experiment employed both limestone and sandstone cores to assess and compare the effectiveness of the neem-derived natural surfactant. The cores' porosity was determined to be 23%, 18% for the two limestone cores, and 19% for Berea sandstone. The absolute permeability values for limestone were 137.7 mD in DIW and 152.5 mD in brine. For sandstone, the permeability values were 141.9 mD in DIW and 240.3 mD in brine.

Considering the importance of establishing a baseline for recovery and true surfactant efficiency, the study evaluated both water-wet and oil-wet systems. Efficiency results were determined with and without the impact of salinity to provide a comprehensive understanding of surfactant performance.

The difference in the impact of the flooding operation is depicted in Fig. 14 and Table 4. During the experiment, the natural surfactant created an emulsion with oil, requiring time for separation and quantity reporting. This created some difficulty in recording the pressure profile and trusting the PV report. However, the operation was concluded based on the step or stage effect. The oil recovery following surfactant injection was approximately 10.2% for limestone and 24% for sandstone when using DIW solution. This notable difference indicates that the surfactant had a more significant impact on oil recovery in the sandstone formation than in the limestone formation in DIW-based conditions, which confirms the anionic nature of the derived surfactant and the impact of adsorption. However, under brine-based conditions, the surfactant injection performed better in the limestone formation, resulting in an oil recovery of 8.3%, whereas the sandstone formation achieved a recovery of only 6.5%.

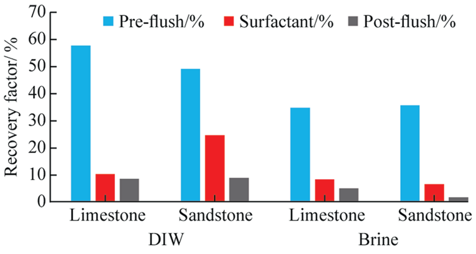

Fig. 14. Comparision of the recovery factor obtained from core flooding under deionized water and brine conditions.

The relationship between pressure drop and flooding typically exhibits a pattern wherein the pressure difference increases and subsequently stabilizes upon the initiation of injection. This phenomenon was observed across all samples—sandstone and limestone, in both saline and non-saline conditions. During surfactant injection, the pressure drop increases further, indicating significant alterations in the system. These pressure increases generally exceed the previous levels. Following surfactant injection, during the water postflush, a pressure surge occurs, presumably due to oil mobilization and formation, after which the pressure gradually decreases. In this experiment, the distinctive feature observed for the sandstone sample flooded with deionized water is the notable pressure oscillation during the post-surfactant phase (Fig. 15). This oscillatory behavior suggests that this data point is particularly sensitive to the mechanisms involved. Some of the previous studies indicated that the surfactant dynamic of self assembly and concentration gradients could result in the insitu heterogeneous flow in some conditions [55,56].

The enhanced efficacy of the natural surfactant in DIW can be attributed to the influence of the chemical composition and ion concentration found in brine. The existence of ions in the brine may impact the behavior and effectiveness of surfactants, resulting in more favorable outcomes in DIW. In the case of brine-based conditions, it was observed that limestone exhibited better performance in oil recovery. This trend continued throughout the experiment, and the limestone sample consistently gathered more oil than the sandstone sample.

Many mechanisms involve in releasing trapped oil during the water/surfactant flooding such as: IFT reduction[33], wettability alteration[57,58], flow path divergence[59,60] and solid/fluid adsorption and fine migrations[61]. However, in a typical setup, the assessment is more influenced by the proven concepts of IFT and wettability alteration. The current study proved that reduction of IFT and adsorption can evidently contribute to the improvement of oil production. However, in DIW, the absence of ions may contribute to increased elasticity at the oil-water interface [62,63], thereby reducing the snap-off of oil droplets. Consequently, this phenomenon results in more uniform oil displacement and higher recovery during the water flooding period. This is particularly more pronounced in sandstone formations where the pore structure and surface charge may better support this process. Furthermore, when the surfactant was injected, the initial surfactant diffusion may have improved interfacial elasticity between oil and water for sandstone and limestone cores. The elasticity theory is less frequently discussed in the literature, although it plays a pivotal role in understanding liquid interactions. The superiority of the results obtained during the water flooding can be explained by the observation of the low ion water content/low salinity role in performing generally better in the first cases recovery [64,65]. When it comes to the sea water salinity, the mechanism attributed

Table 4
Core flooding results.

Parameters	Units	Limestone	Sandstone	Limestone	Sandstone
		DIW		Brine	
Natural surfactant viscosity at 25 °C	cP	1.2		1.18	
Natural surfactant concentration	wt%	4.2		1.1	
Salinity	ppm	0		35,000	
Permeability to oil	mD	67.2	96.4	66.7	147.6
Water breakthrough after (PV injected)	mL	11.8	11.4	14.4	12.4
Recovery from initial WF 5 PV	%	57.6	49.1	34.7	35.5
Additional recovery after 1 PV of Nat. surfactant	%	12.0	11.0	8.3	6.5
Additional recovery after the final WF (5 PV)	%	10.2	24.6	4.9	1.6
Estimated water saturation	%	39.7	31.7	8.8	22.9

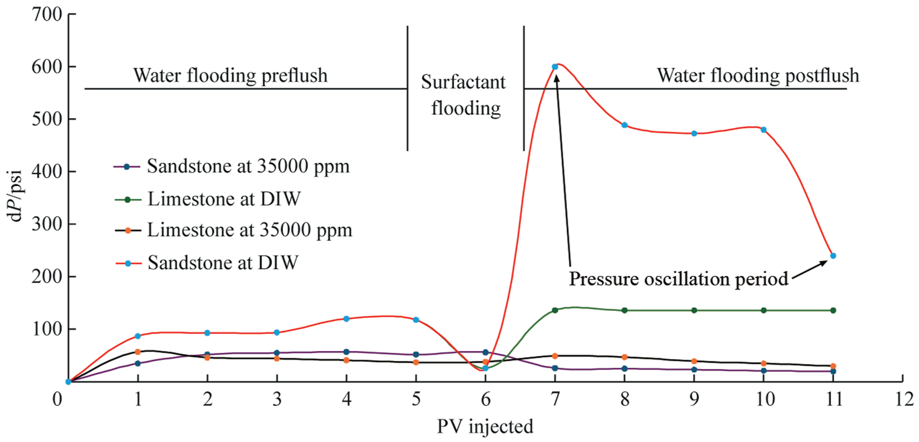

Fig. 15. Pressure drop profile.

to the recovery differs. In the research conducted by Hou et al. [66], the higher the salinity, the higher the surfactant adsorption. This positively influences the alteration of calcite surface wettability. Additionally, the differences include rock properties, wettability alteration, pore structure, mineralogy, surface charge, salinity, and ionic strength.

4. Conclusions

This research aimed to investigate the viability and effectiveness of employing natural surfactants to enhance oil recovery. The neem-derived surfactant validated the existence of saponin and triterpenoid by FTIR. Scanning electron microscope analysis revealed irregularities in the morphology of the surfactant, characterized by varying shapes and sizes. The observed surfactant particles ranged in size from 80 μm to 500 μm. The EDS confirmed the presence of Na, which asserts the surfactant's saponification, converting fatty acid esters to sodium salts, indicating its anionic properties in water. The ST measurement in DIW and brine confirmed the nature of the surface activity, with a notable decrease in IFT as the concentration increased from 1 wt% to 6 wt%. The IFT dropped from 22.5 mN/m to 7.9 mN/m, reflecting a remarkable 64.8% decrease. Surfactants form micelles more efficiently in saline water, with CMC dropping from 4.0 wt% in DIW to 0.9 wt%. This can support the future economic viability since the required concentration is lowered by 77.5%. For optimal salinity evaluation, it is seen that increasing salinity reduces IFT until 1.5 wt%, beyond which it is less significant. At sea water salinity, the IFT stabilizes, indicating saturation on the oil–water interface. Neem-derived surfactant tolerates seawater salinity but is not optimal for maximum IFT reduction. Observing the temperature range in Kazakhstan revealed that the surfactant maintains its effectiveness across the temperature spectrum examined. However, observations of the high concentrations suggested it is more likely that increasing the temperature reduced the IFT. The concerns about natural surfactant adsorption showed that limestone has >50% higher adsorption capacity than sandstone due to its hydrophobic nature and the natural surfactant's anionic properties.

Evaluating the natural surfactant's effectiveness through core flooding experiments assessed oil and water-wet conditions. Oil-wet limestone exhibited a reduction in water flooding recovery by 23% from DIW to saline conditions, while water-wet sandstone was reduced by 14%. When no salinity was introduced, the recovery attributed to natural surfactant was 22% and 34% for limestone and sandstone, respectively. In saline conditions, the limestone showed a recovery of 13%, while 8% was achieved by sandstone. This is attributed to surfactant adsorption on limestone and further improving the transioning to water-wet. In conclusion, the natural surfactant extracted demonstrates considerable potential for enhancing production across various conditions, indicating favorable prospects for its future implementation in Kazakhstan's oil fields. However, for future implementation, the field crude should be utilized to ensure direct applicability of the results to actual reservoir conditions. Subsequent research should focus on evaluating the surfactant with real crude oil samples from Kazakhstan to more accurately assess its performance in more representative environments. The study offered insights that lead to innovative EOR strategies, promoting a more sustainable approach in the oil and gas industry while minimizing environmental impacts.

CRediT authorship contribution statement

Aibike Tukhfatova: Investigation, Formal analysis. **Azza Hashim Abbas:** Funding acquisition, Conceptualization, Investigation, Writing – review & editing. **Sonny Irawan:** Supervision. **Peyman Pourafshary:** Writing – review & editing.

Declaration of competing interest

The authors declare there is no financial interests/personal relationships which may be considered as potential competing or conflict of interests.

Acknowledgment

The authors would like to thank Nazarbayev University for supporting this research through the NU Faculty Development Competitive Research Grants Program (Grant numbers: 20122022FD4137 (AHA).The authors would like to thank Aizahn Rakhimnova for her support during the characterization process.

Appendix A. Supplementary data

Supplementary data to this article can be found online at https://doi.org/10.1016/j.petlm.2025.09.001.

References

[1] A. Jordan, D. Daulton, J. Ann Cobb, T. Grumbles, Quantitative ranking measures oil field chemicals environmental impact, in: SPE Annual Technical Conference and Exhibition?, 2010. SPE, SPE-135517-MS.

[2] S. Taj, S. Papavinasam, R.W. Revie, Development of Green Inhibitors for Oil and Gas Applications, NACE CORROSION, 2006. NACE, NACE-06656.

[3] S. Rellegadla, G. Prajapat, A. Agrawal, Polymers for enhanced oil recovery: fundamentals and selection criteria, Appl. Microbiol. Biotechnol. 101 (2017) 4387–4402.

[4] H. Guo, M. Dou, W. Hanqing, F. Wang, G. Yuanyuan, Z. Yu, W. Yansheng, Y. Li, Review of capillary number in chemical enhanced oil recovery, in: SPE Kuwait Oil and Gas Show and Conference, SPE, 2015. SPE-175172-MS.

[5] J.R.,C. Johnson, Evaluation of surfactants for oil field flooding, JAOCS (J. Am. Oil Chem. Soc.) 34 (1957) 209–214.

[6] G.D. Ortloff, New Recovery Methods—Their Prospects and Limitations, 1960.

[7] W. Gogarty, Status of surfactant or micellar methods, J. Petrol. Technol. 28 (1976) 93–102.

[8] G. Pope, B. Wang, K. Tsaur, A sensitivity study of micellar/polymer flooding, Soc. Petrol. Eng. J. 19 (1979) 357–368.

[9] G.A. Pope, K. Tsaur, R.S. Schechter, B. Wang, The effect of several polymers on the phase behavior of micellar fluids, Soc. Petrol. Eng. J. 22 (1982) 816–830.

[10] A. Michels, R. Djojosoeparto, H. Haas, R. Mattern, P. VAN DER Weg, W. Schulte, Enhanced waterflooding design with dilute surfactant concentrations for North Sea conditions, SPE Reserv. Eng. 11 (1996) 189–195.

[11] D.Y. Atta, B.M. Negash, N. Yekeen, A.D. Habte, A state-of-the-art review on the application of natural surfactants in enhanced oil recovery, J. Mol. Liq. 321 (2021) 3–24.

[12] Z. Bachari, A.A. Isari, H. Mahmoudi, S. Moradi, E.H. Mahvelati, Application of Natural Surfactants for Enhanced Oil Recovery – Critical Review, 2019 012074.

[13] M. Norouzpour, M. Nabipour, A. Azdarpour, H. Akhondzadeh, R.M. Santos, A. Keshavarz, Experimental investigation of the effect of a quinoa-derived saponin-based green natural surfactant on enhanced oil recovery, Fuel 318 (2022) 123652.

[14] M. Norouzpour, M. Nabipour, A. Azdarpour, H. Akhondzadeh, R.M. Santos, A. Keshavarz, Experimental investigation of the effect of a quinoa-derived saponin-based green natural surfactant on enhanced oil recovery, Fuel 318 (2022) 1–15.

[15] M. Yusuf, M.H. Wathon, V. Thanasaksukthawee, A. Saul, S. Tangparitkul, Adsorption of saponin natural surfactant on carbonate rock and comparison to synthetic surfactants: an enhanced oil recovery prospective, Energy Fuel. 35 (2021) 11193–11202.

[16] M.S. Almutairi, M. Ali, Direct detection of saponins in crude extracts of soapnuts by FTIR, Nat. Prod. Res. 29 (2015) 1271–1275.

[17] A.B. Chhetri, K.C. Watts, M.S. Rahman, M.R. Islam, Soapnut extract as a natural surfactant for enhanced oil recovery, Energy Sources, Part A Recovery, Util. Environ. Eff. 31 (2009) 1893–1903.

[18] N. Yekeen, A.A. Malik, A.K. Idris, N.I. Reepei, K. Ganie, Foaming properties, wettability alteration and interfacial tension reduction by saponin extracted from soapnut (Sapindus Mukorossi) at room and reservoir conditions, J. Petrol. Sci. Eng. 195 (2020) 107591.

[19] A.H. Abbas, R.A. Abd Alsaheb, J.K. Abdullah, Comparative study of natural chemical for enhanced oil recovery: focus on extraction and adsorption at quartz sand surface, Petroleum 9 (1) (2023) 83–93.

[20] A. Nafisifar, A.K. Manshad, S.R. Shadizadeh, Evaluation of a new green synthesized surfactant from linseeds - chemical EOR implications from sandstone petroleum reservoirs, J. Mol. Liq. 342 (2021).

[21] L. Zhao, Y. Guo, A. Azdarpour, E. Mohammadian, M. Norouzpour, B. Liu, Synergism of a novel bio-based surfactant derived from pisum sativum and formation brine for chemical enhanced oil recovery in carbonate oil reservoirs, Processes 11 (2023) 1361.

[22] A.H. Abbas, N. Keldibayev, P. Pourafshary, Y. Zhuniskenov, G. Serikov, Numerical simulation of flaxseed gum potential in improving oil recovery: focus on offshore Kazakhstan, in: Offshore Technology Conference Asia, OTC, 2024 D021S014R005.

[23] Y. Zhuniskenov, A. Sabirova, G. Serikov, A.H. Abbas, P. Pourafshary, Impact of the naturally driven surfactant in EOR application: experimental, microscopic, and numerical analyses, ACS Omega 9 (2023) 1327–1340.

[24] G. Serikov, A. Hashim, P. Pourafshary, Y. Zhuniskenov, M. Mohyaldinn, Vitality of natural polymers in safe flooding in offshore operation: road to Caspian Sea implementation, in: Offshore Technology Conference Asia, OTC, 2024. D021S010R007.

[25] M. Eslahati, P. Mehrabianfar, A.A. Isari, H. Bahraminejad, A.K. Manshad, A. Keshavarz, Experimental investigation of Alfalfa natural surfactant and synergistic effects of Ca2+, Mg2+, and SO42− ions for EOR applications: interfacial tension optimization, wettability alteration and imbibition studies, J. Mol. Liq. 310 (2020) 113123.

[26] S.R.M. Dashtaki, J.A. Ali, A.K. Manshad, I. Nowrouzi, A.H. Mohammadi, A. Keshavarz, Experimental investigation of the effect of Vitagnus plant extract on enhanced oil recovery process using interfacial tension (IFT) reduction and wettability alteration mechanisms, J. Pet. Explor. Prod. Technol. 10 (2020) 2895–2905.

[27] I. Nowrouzi, A.H. Mohammadi, A.K. Manshad, Characterization and evaluation of a natural surfactant extracted from Soapwort plant for alkali-surfactant-polymer (ASP) slug injection into sandstone oil reservoirs, J. Mol. Liq. 318 (2020) 114369.

[28] H. Kesarwani, A. Saxena, N. Saxena, S. Sharma, Oil mobilization potential of a novel anionic karanj oil surfactant: interfacial, wetting characteristic, adsorption, and oil recovery studies, Energy Fuel. 35 (2021) 10597–10610.

[29] I. Nowrouzi, A.H. Mohammadi, A. Khaksar Manshad, Preliminary evaluation of a natural surfactant extracted from Myrtus communis plant for enhancing oil recovery from carbonate oil reservoirs, J. Pet. Explor. Prod. Technol. 12 (2022) 783–792.

[30] S.R. Shadizadeh, S.R. Seyedi Abandankashi, S. Moradi, Experimental investigation used of albizia julibrissin extract as a plant surfactant on oil recovery, Iranian Journal of Oil and Gas Science and Technology 10 (2021) 89–106.

[31] H. Imuetinyan, A. Agi, A. Gbadamosi, R. Junin, J. Oseh, Oil-water interfacial tension, wettability alteration and foaming studies of natural surfactant extracted from Vernonia Amygdalina, Petroleum Research 7 (2022) 350–356.

[32] S.R.M. Dashtaki, J.A. Ali, B. Majeed, A.K. Manshad, I. Nowrouzi, S. Iglauer, A. Keshavarz, Evaluation the role of natural surfactants from Tanacetum and Tarragon plants in EOR applications, J. Mol. Liq. (2022) 119576.

[33] L. Yisong, R. Gholami, M. Safari, A. Rahimi, W.S. Khur, On surface interactions of environmental friendly surfactant/oil/rock/low salinity system: IFT, wettability, and foamability, J. Petrol. Sci. Eng. 208 (2022) 109370.

[34] A.A. Obuebite, W.I. Eke, T. Udoh, Evaluation of modified cashew nutshell liquid as natural surfactants for chemical flooding in sandstone oil reservoirs, J. Eng. Appl. Sci. 69 (2022) 114.

[35] M.N. Nwanekezie, J.N. Ndive, I.L. Ogbonna, G.O. Sebe, Comprehensive physicochemical profiling and characterization of neem plant leaf extracts: insights for pharmaceutical & biomedical applications, Adv. Chem. Eng. Sci. 13 (2023) 382–399.

[36] A. Rohman, Y. Man, Fourier transform infrared (FTIR) spectroscopy for analysis of Extra Virgin Oil adulterated with palm Oil, Food Res. Int. 43 (2010) 886–892.

[37] R.S. Irnawati, S. Martono, A. Rohman, Analysis of palm oil as oil adulterant in olive and pumpkin seed oils in ternary mixture systems using FTIR spectroscopy and chemometrics, Int. J. Appl. Pharm. 11 (2019) 210–215.

[38] S. Ahmed, M. Ahmad, B.L. Swami, S. Ikram, Green synthesis of silver nanoparticles using Azadirachta indica aqueous leaf extract, Journal of radiation research and applied sciences 9 (2016) 1–7.

[39] A. Hameed, T.U. Rehman, Z.A. Rehan, R. Noreen, S. Iqbal, S. Batool, M. A. Qayyum, T. Ahmed, T. Farooq, Development of polymeric nanofibers blended with extract of neem (Azadirachta indica), for potential biomedical applications, Frontiers in Materials 9 (2022) 1042304.

[40] O. Uncu, B. Ozen, F. Tokatli, Use of FTIR and UV–visible spectroscopy in determination of chemical characteristics of olive oils, Talanta 201 (2019) 65–73.

[41] T. Ogunkunle, A. Fadairo, V. Rasouli, K. Ling, A. Oladepo, O. Chukwuma, J. Ayoo, Microbial-derived bio-surfactant using neem oil as substrate and its suitability for enhanced oil recovery, J. Pet. Explor. Prod. Technol. 11 (2021) 627–638.

[42] C.S. DE Azevedo Sá, R. Ladchumananandasivam, C.G.F.T. Rossi, R.K. Da Silva, W.D.S. Camboim, A. Zille, J. Padrão, K.K. DE Oliveira Souto Silva, Characterization of a natural surfactant from an essential oil from neem (Azadirachta indica A. Juss) for textile industry applications, Textil. Res. J. 92 (2021).

[43] P. Lai, K. Moulton, S. Krevor, Pore-scale heterogeneity in the mineral distribution and reactive surface area of porous rocks, Chem. Geol. 411 (2015) 260–273.

[44] H.S. EL-Sheshtawy, I. Aiad, M.E. Osman, A.A. Abo-Elnasr, A.S. Kobisy, Production of biosurfactant from Bacillus licheniformis for microbial enhanced oil recovery and inhibition the growth of sulfate reducing bacteria, Egypt. J. Pet. 24 (2015) 155–162.

[45] R. Muneer, R. Alimkulov, N. Eghtesadi, A. Ormantayeva, T. Thanh Pham, A. H. Abbas, Micellization behavior and thermodynamic characteristics of saponin and SDS: the impact of silica nanoparticles for subsurface formation interaction studies, ChemistrySelect 9 (2024) e202305102.

[46] A. Wołowicz, K. Staszak, Study of surface properties of aqueous solutions of sodium dodecyl sulfate in the presence of hydrochloric acid and heavy metal ions, J. Mol. Liq. 299 (2020) 112170.

[47] A.H. Abbas, A. Moslemizadeh, W.R.W. Sulaiman, M.Z. Jaafar, A. Agi, An insight into a di-chain surfactant adsorption onto sandstone minerals under different salinity-temperature conditions: chemical EOR applications, Chem. Eng. Res. Des. 153 (2019).

[48] A.H. Abbas, W.R.W. Sulaiman, M.Z. Jaafar, A.A. Aja, Micelle formation of Aerosol-OT surfactants in Sea water salinity, Arabian J. Sci. Eng. (2017) 1–5.

[49] N. Yekeen, M.A. Manan, A.K. Idris, A.M. Samin, Influence of surfactant and electrolyte concentrations on surfactant adsorption and foaming characteristics, J. Petrol. Sci. Eng. 149 (2017) 612–622.

[50] R.K. Saw, P.M. Rane, D. Joshi, S. Prakash, L. Jangid, A. Mandal, Enhanced oil recovery using a novel non-ionic surfactant synthesized from olive oil: performance and synergistic effects, J. Mol. Liq. 392 (2023) 123452.

[51] H. Khayati, A. Moslemizadeh, K. Shahbazi, M. Keshavarz Moraveji, S.H. Riazi, An experimental investigation on the use of saponin as a non-ionic surfactant for chemical enhanced oil recovery (EOR) in sandstone and carbonate oil reservoirs: IFT, wettability alteration, and oil recovery, Chem. Eng. Res. Des. 160 (2020) 417–425.

[52] N. Akhlaghi, S. Riahi, R. Parvaneh, Interfacial tension behavior of a nonionic surfactant in oil/water system; salinity, pH, temperature, and ionic strength effects, J. Petrol. Sci. Eng. 198 (2021).

[53] E.J. Behrens, Investigation of Loss of Surfactants During Enhanced Oil Recovery applications-adsorption of Surfactants onto Clay Materials, Norwegian University of Science and Technology, 2013. MSc. Degree in Industrial Chemistry and Biotechnology Thesis.

[54] A.H. Abbas, A. Moslemizadeh, W.R.W. Sulaiman, M.Z. Jaafar, P. Pourafshary, Lignin adsorption in sandpacks during horizontal flow using UV–Vis spectrometry as a quantification tool, Arabian J. Geosci. 15 (2022) 501.

[55] M. Roché, Z. Li, I.M. Griffiths, S. LE Roux, I. Cantat, A. Saint-Jalmes, H.A. Stone, Marangoni flow of soluble amphiphiles, Phys. Rev. Lett. 112 (2014) 208302.
[56] S. Kahrobaei, R. Farajzadeh, Insights into Effects of Surfactant Concentration on Foam Behavior in Porous Media. IOR 2019–20th European Symposium on Improved Oil Recovery, European Association of Geoscientists & Engineers, 2019, pp. 1–13.
[57] M. Amirmoshiri, L. Zhang, M.C. Puerto, R.D. Tewari, R. Bahrim, R. Farajzadeh, G.J. Hirasaki, S.L. Biswal, Role of wettability on the adsorption of an anionic surfactant on sandstone cores, Langmuir 36 (2020) 10725–10738.
[58] T. Puntervold, T. Austad, Injection of seawater and mixtures with produced water into North Sea chalk formation: impact of fluid–rock interactions on wettability and scale formation, J. Petrol. Sci. Eng. 63 (2008) 23–33.
[59] A.H. Abbas, W.R.W. Sulaiman, M.Z. Jaafar, A.A. Agi, Laboratory experiment based permeability reduction estimation for enhanced oil recovery, J. Eng. Sci. Technol. 13 (2018) 2464–2480.
[60] D. Abraham, O. Orodu, V. Efeovbokhan, O. Ee, T. Ojo, E. Bolujo, Evaluation of permeability impairment due to surfactant flooding, in: IOP Conference Series: Earth and Environmental Science, IOP Publishing, 2021 012065.
[61] R.A. Nasralla, H.A. Nasr-EL-Din, Impact of electrical surface charges and cation exchange on oil recovery by low salinity water, in: SPE Asia Pacific Oil and Gas Conference and Exhibition, 2011. SPE, SPE-147937-MS.
[62] L. Rosenfeld, G.G. Fuller, Consequences of interfacial viscoelasticity on thin film stability, Langmuir 28 (2012) 14238–14244.
[63] T.S.E. Chávez-Miyauchi, A. Firoozabadi, G.G. Fuller, Nonmonotonic elasticity of the crude oil–brine interface in relation to improved oil recovery, Langmuir 32 (2016) 2192–2198.
[64] T. Kar, T.S.-E. Chávez-Miyauchi, A. Firoozabadi, M. Pal, Improved oil recovery in carbonates by ultralow concentration of functional molecules in injection water through an increase in interfacial viscoelasticity, Langmuir 36 (2020) 12160–12167.
[65] T. Kar, H. Cho, A. Firoozabadi, Assessment of low salinity waterflooding in carbonate cores: interfacial viscoelasticity and tuning process efficiency by use of non-ionic surfactant, J. Colloid Interface Sci. 607 (2022) 125–133.
[66] J. Hou, S. Lin, J. Du, H. Sui, Study of the adsorption behavior of surfactants on carbonate surface by experiment and molecular dynamics simulation, Front. Chem. 10 (2022).